



UNIVERSITY OF LEEDS

This is a repository copy of *Magneto-thermodynamic properties and anomalous magnetic phase transition in FeRh nanowires*.

White Rose Research Online URL for this paper:

<https://eprints.whiterose.ac.uk/130028/>

Version: Accepted Version

Article:

Matsumoto, K orcid.org/0000-0002-3433-2041, Kimata, M orcid.org/0000-0003-4936-2988, Kondou, K orcid.org/0000-0002-3020-3189 et al. (3 more authors) (2018)

Magneto-thermodynamic properties and anomalous magnetic phase transition in FeRh nanowires. IEEE Transactions on Magnetics, 54 (11). ARTN 2300904. ISSN 0018-9464

<https://doi.org/10.1109/TMAG.2018.2832191>

© 2018 IEEE. Personal use of this material is permitted. Permission from IEEE must be obtained for all other uses, in any current or future media, including reprinting/republishing this material for advertising or promotional purposes, creating new collective works, for resale or redistribution to servers or lists, or reuse of any copyrighted component of this work in other works.

Reuse

Items deposited in White Rose Research Online are protected by copyright, with all rights reserved unless indicated otherwise. They may be downloaded and/or printed for private study, or other acts as permitted by national copyright laws. The publisher or other rights holders may allow further reproduction and re-use of the full text version. This is indicated by the licence information on the White Rose Research Online record for the item.

Takedown

If you consider content in White Rose Research Online to be in breach of UK law, please notify us by emailing eprints@whiterose.ac.uk including the URL of the record and the reason for the withdrawal request.



eprints@whiterose.ac.uk
<https://eprints.whiterose.ac.uk/>

Magneto-thermodynamic properties and anomalous magnetic phase transition in FeRh nanowires

K. Matsumoto¹, M. Kimata¹, K. Kondou², R. C. Temple³, C. H. Marrows³ and Y. Otani^{1, 2}

¹Institute for Solid State Physics, the University of Tokyo, Kashiwa, Chiba 277, Japan

²Center for Emergent Matter Science, RIKEN, Wako, Saitama 351, Japan

³School of Physics and Astronomy, University of Leeds, Leeds, LS2 9JT, UK

Thermal properties of submicron wires of Pd-doped FeRh alloys are evaluated from measurements of transport properties around the first order antiferromagnetic to ferromagnetic phase transition. Recently, in a submicron wire of FeRh alloy, an asymmetric structure between heating and cooling processes was reported in the vicinity of the phase transition temperature. A system where finite-size effects appear is expected to show different magnetic and thermal properties from those in bulk and thin film. However, thermal or magnetization measurements are difficult to perform on samples with such a tiny volume. Here, we demonstrate a quantitative evaluation of thermal properties in thin films and submicron wires of B2-ordered Pd-doped FeRh alloy grown on MgO (001). Resistivity measurements on a series of wires with different width reveal that the anomaly in the resistance change is enhanced in narrow wires. As the transport properties in submicron wires sensitively reflect those magnetic states, the entropy change and irreversible energy loss during the first order phase transition have been determined via resistance measurements. We find a larger energy loss in smaller samples where wider hysteresis loops appear in temperature-driven measurements. This method can be a probe to evaluate the finite-size effect induced by a restricted magnetic domain nucleation process during the phase transition.

Index Terms—FeRh alloys, first order phase transition, metamagnetic transition, thin films, submicron wires.

I. INTRODUCTION

THE FeRh ALLOY with B2 order shows a first order phase transition from an antiferromagnetic (AFM) to a ferromagnetic (FM) phase with rising temperature at around 370 K [1]. This phase transition is accompanied by a large change in longitudinal and Hall resistivity [2]–[4], lattice constant [5] and entropy [6], [7]. The transition temperature is tunable around room temperature by a control of chemical composition [8], [9], so FeRh alloys are candidate materials for several applications such as heat-assisted magnetic recording [10], [11], AFM memories [12], [13], and memristor devices [14].

Recently, asymmetric behavior around the AFM – FM phase transition of FeRh alloys has been reported on some tiny sample structures, such as ultra-thin films with an island-like morphology [15] and nanoparticles [16]. Remarkably, a discontinuous and asymmetric resistance change around the phase transition was reported in submicron wires of FeRh alloy [17], [18]. This anomalous behavior is caused by suppression of the nucleation process of antiferromagnetic domains during the cooling process [18], which is also expected to make a significant difference to the thermal properties. Evaluation of thermal quantities would enable a quantitative characterization of finite-size effects around the phase transition. However, it is difficult to conduct volume-sensitive thermal or magnetization measurements on such small volume samples.

In FeRh alloys, it is possible to estimate those thermal properties indirectly around the metamagnetic phase transition. The transition temperature is suppressed under the application of external magnetic field because of the reduction of the free energy of the FM phase [19]. This transition temperature suppression by an external field enables the derivation of some

thermodynamic parameters from magnetization measurements [20], [21], which gives consistent results with thermal measurements [2], [7]. From these reports, it is known that both a bulk specimen and a thin film of FeRh exhibit similar transition temperatures and entropy changes.

Here, we performed resistivity measurements of submicron wires of FeRh as a function of temperature and external magnetic field. As the resistance change in a submicron specimen reflected local magnetic states, difference in entropy between the two phases and energy loss due to temperature hysteresis were estimated from electrical transport measurements.

II. EXPERIMENTAL TECHNIQUE

Films of Pd-doped FeRh alloys were prepared by DC magnetron sputtering from an $\text{Fe}_{47}\text{Rh}_{50}\text{Pd}_3$ alloy target. 60 nm thick films were grown on top of MgO (001) substrates at 600°C and annealed in situ at 700°C for 1 hour after the deposition. In order to improve the chemical ordering of the alloy, the films were annealed again in vacuum at 800°C for 2 hours. X-ray diffraction patterns of the film after the thermal treatments revealed B2-ordered chemical structure and FeRhPd (001) orientation on MgO (001).

Magnetization measurements of FeRhPd films were performed in a superconducting quantum interference device magnetometer in a temperature range from 100 to 340 K under in-plane external magnetic field. Submicron wires were fabricated by a combination of electron beam lithography and Ar ion milling. 150 nm thick Cu electrodes were patterned on top of the wires and deposited by electron beam evaporation. Four- or two-terminal resistance measurements using a Quantum Design PPMS were performed with an excitation current of 500 nA, which is small enough to avoid the transition to the high-temperature phase activated by Joule

heating effect onto the small volume specimen [13], [22].

III. RESULTS AND DISCUSSION

A. Magnetization and Entropy Change in Unpatterned Films

Fig. 1 (a) shows a temperature loop of magnetization on an FeRhPd film with application of an in-plane magnetic field of 0.1 T. The magnetization exhibited a saturated value

$$\frac{dM}{dT} \bigg|_{T_{tr}} \left(\frac{dM}{dH_{ext}} \right)$$

of in high-temperature FM phase and disappeared in low-temperature AFM phase. Residual magnetization originating from the vicinity of interface was $1.1 \times 10^4 \text{ A}\cdot\text{m}^{-1}$ below transition temperature. Because of the elemental substitution effect due to a Pd doping [9], the phase transition temperature of FeRhPd films was decreased to around room temperature whereas that of an equiatomic FeRh alloy is around 370 K [1]. As the $M - T$ trace makes a temperature hysteresis loop on heating and cooling arms, two transition temperatures can be determined corresponding to the two arms. Here we define transition temperatures T_{AFM-FM} and T_{FM-AFM} as temperatures where the maximum points of the first derivative of $M - T$ curves appears on heating and cooling processes, respectively. Under an external magnetic field of 0.1 T, T_{AFM-FM} was 297.7 K and T_{FM-AFM} was 276.9 K.

The magnetization of the unpatterned FeRhPd film was measured with sweeping temperature under a series of constant in-plane magnetic fields between 0.05 and 1.5 T. T_{AFM-FM} and T_{FM-AFM} were plotted against the applied in-plane magnetic field in Fig. 1 (b). The width of a temperature hysteresis loop was constant in different external magnetic fields, which is consistent with previous reports [20], [23]. Both of two transition temperatures showed linear decreases against an application of external magnetic field with a slope of . As this linear decrease is caused by a decrease in FM phase free energy, the released entropy accompanying the

phase transition can be estimated as [20]

(1)

Here T_{tr} is an averaged transition temperature of T_{AFM-FM} and T_{FM-AFM} , ΔM is change in magnetization during the transition, and ΔS is the entropy change between FM and AFM phases. For our experimentally determined values of the slope and magnetization, the entropy change in the film was estimated to

be , which is comparable to the reported values for a bulk specimen [2] () and a thin film [20] ().

FIG. 1 HERE

B. Resistance and Entropy Change in Submicron Wires

The entropy change ΔS accompanied with AFM - FM phase transition was determined via magnetization measurements of the unpatterned FeRhPd film whereas a

submicron wire has a difficulty on volume-sensitive magnetization measurements. In this section, ΔS in the patterned wire is characterized through electrical transport measurements.

Four-terminal resistance measurement was performed on a 270 nm wide wire with sweeping temperature or in-plane

magnetic field as shown in Fig. 2. The inset of Fig. 2 exhibits a SEM image of the wire specimen and attached Cu electrodes. The temperature-driven measurement showed the phase transition at around 280 K, whereas the film specimen before fabrication exhibited a higher transition temperature around 295 K. This decrease in the transition temperature was seen in all submicron wires of different widths, so it could be influenced by the fabrication process such as Ar ion milling. Both of $R - T$ and $R - B$ traces showed quite similar hysteresis shape including large discontinuous resistance changes during the transition from FM to AFM phase, which is a characteristic behavior in submicron wires [18]. This asymmetry is caused by a suppression of the nucleation process of AFM domains. The similarity in the field- and temperature-driven transport measurements indicates that, even in submicron wires, those thermal properties can be represented as a linear function of temperature and external magnetic field in the vicinity of AFM - FM phase transition.

The largest resistance change during the transition from FM to AFM phase occurred at 0 T and 256.6 K in a temperature-driven measurement, and at 240.0 K and 1.46 T in a field-driven measurement. As the traces showed 60.7% of total

resistance change at both the two points, we assumed the transition volume is same on these points. Then, ΔS could be derived from the evaluation of released energy accompanied with the transition.

FIG. 2 HERE

The latent heat exported during the transition from the high-temperature to the low-temperature phase is $T\Delta S$. Under an external magnetic field H , the Zeeman energy term $\mu_0 H \Delta M$ also contributes to the energy release during the phase transition. The sum of the latent heat $T\Delta S$ and Zeeman energy term $\mu_0 H \Delta M$ represents the total exported energy during the temperature- or field-driven phase transition. Under the assumption that the released energy is equivalent in both temperature- and field-driven measurements at the two points referred to, entropy change in the wire is derived as . This value is smaller than the one estimated in the same film before fabrication

(). This difference may be related to the change in transition temperature of submicron wires. Kushwaha *et al.* reported a large sensitivity to an external field, , on Pd-doped FeRh films which exhibit phase transition around 200 K [23]. This would suggest a tendency that differences of entropy between AFM and FM phases are smaller when the transition occurs at lower

temperatures.

C. Evaluation of Energy Loss

Because both the unpatterned film and submicron wires showed closed hysteresis loops with sweeping temperature, there exists a finite irreversible energy loss Q'' around the AFM – FM phase transition for each specimen. As the energy loss is characterized by the temperature hysteresis loop, it can be a quantitative index for representing the size of the finite-size effect. Q'' is equal to the integrated entropy around a temperature hysteresis loop, so it can be calculated from $M - T$ plot:

$$Q'' = \int_{T_1}^{T_2} (M_{AFM} - M_{FM}) dT \quad (2)$$

Here we used eq. (1) and assumed ΔS is not temperature dependent in the vicinity of transition temperature. From the calculation of the $M - T$ hysteresis area of the unpatterned film shown in Fig. 1 (a), we obtained

Though it is difficult to measure the magnetization of a sample with a tiny volume, estimation of the FM volume ratio in a submicron wire is possible from electrical transport measurements. In a small range of temperature around the phase transition, resistivity in AFM or FM phase can be approximated to be a linear function of temperature. As the width of submicron wires are comparable to the size of magnetic domains observed on films of FeRh alloys [24], [25], we assumed AFM and FM domains in wire structures are aligned along the longitudinal direction of the wire. Under this assumption, sample resistance $R(T)$ can be represented by a linear combination of the resistances in two phases as follows:

$$R(T) = x R_{FM}(T) + (1-x) R_{AFM}(T) \quad (3)$$

Here x is a volume ratio of FM domains in the wire sample, $R_{FM}(T)$ and $R_{AFM}(T)$ are wire resistances where all volume of the sample exhibits FM and AFM phases, respectively. They are extrapolated from $R - T$ traces above and below the temperature hysteresis.

Temperature-driven resistance measurements without external magnetic field were performed on wires with different widths of 270 nm, 660 nm, and 1160 nm. From X-ray magnetic circular dichroism and photoemission electron microscopy measurements on FeRh films, the typical domain size around the transition temperature was revealed to be about 550 nm for FM domains and 300 nm or less for AFM domains [25]. In this range of wire sizes, it is expected to exhibit some difference due to finite-size effects. Fig. 3 shows the estimated FM volume ratio against temperature for each wire. The anomaly in the resistance change was enhanced in the small wires. The symmetric and continuous change in resistance of the widest one would suggest a disappearance of finite-size effects.

FIG. 3 HERE

As the FM volume ratio x is equivalent to $\frac{R_{AFM}(T) - R(T)}{R_{AFM}(T) - R_{FM}(T)}$,

energy loss can be represented as $Q'' = \int_{T_1}^{T_2} (M_{AFM} - M_{FM}) dT$ in submicron wires. Here we assumed the decrease in entropy change was originated from a shift in transition temperature. As the transition temperatures are same in the three wires, a value of ΔS estimated in 270 nm wide wire, 113

$\text{J}\cdot\text{cm}^{-3}$, was used for all wires. We finally obtained energy loss of $3.39 \text{ J}\cdot\text{cm}^{-3}$, $3.31 \text{ J}\cdot\text{cm}^{-3}$, and $3.08 \text{ J}\cdot\text{cm}^{-3}$ for the wires with a width of 270, 660, and 1160 nm. Even the entropy change in wires is smaller than that of unpatterned film, energy loss around the AFM – FM transition was larger than $3.08 \text{ J}\cdot\text{cm}^{-3}$ in the film. It also showed a tendency that energy loss was larger in a smaller specimen due to its wider hysteresis width. As the asymmetry in hysteresis loop is thought to be caused by the domain nucleation process, this result would be an evidence to show the contribution of magnetic domain structures across the phase transition to the macroscopic energy loss.

IV. CONCLUSION

In this work, we performed electrical transport measurements on submicron wires of Pd-doped FeRh alloys. As the resistance on a submicron specimen reflects local magnetic states, entropy change ΔS and hysteresis energy loss Q'' were estimated from electrical measurements. ΔS in a submicron wire was $3.39 \text{ J}\cdot\text{cm}^{-3}$, which was smaller than that in the unpatterned film, $3.08 \text{ J}\cdot\text{cm}^{-3}$. This decrease in the entropy change would be related to the lower transition temperature in wires. In a comparison of temperature-driven resistance changes in a series of wires of different sizes, the anomalous asymmetry in hysteresis loop was found to be enhanced in the smallest wire. We also found a change in the irreversible energy loss between the submicron wires and the film. The energy loss was enlarged in a smaller sample, which suggests that the finite-size effect, probably a change in magnetic domain structures across the phase transition, appears in a macroscopic property. We demonstrated a quantitative evaluation of an influence of domain nucleation process to the magnetic states in submicron wires by simple electrical $M(T)$ measurements.

ACKNOWLEDGMENT

This work is supported by a Grant-in-aid for Scientific Research on Innovative Area, “Nano Spin Conversion Science” (Grant No. 26103002) and by the EPSRC through grant number EP/M018504/1. Data associated with the EPSRC-funded parts of this work are available at <https://doi.org/10.5518/338>.

REFERENCES

- [1] J. S. Kouvel and C. C. Hartelius, “Anomalous magnetic moments and transformations in the ordered alloy FeRh,” *J. Appl. Phys.*, vol. 33, no. 3, pp. 1343–1344, 1962.
- [2] J. S. Kouvel, “Unusual nature of the abrupt magnetic transition in FeRh and its pseudobinary variants,” *J. Appl. Phys.*, vol. 37, no. 3, pp. 1257–1258, 1966.

- [3] Y. Kobayashi, K. Muta, and K. Asai, "The Hall effect and thermoelectric power correlated with the giant magnetoresistance in modified FeRh compounds," *J. Phys. Condens. Matter*, vol. 13, no. 14, pp. 3335–3346, Apr. 2001.
- [4] M. A. De Vries, M. Loving, a. P. Mihai, L. H. Lewis, D. Heiman, and C. H. Marrows, "Hall-effect characterization of the metamagnetic transition in FeRh," *New J. Phys.*, vol. 15, p. 13008, 2013.
- [5] M. A. De Vries *et al.*, "Asymmetric „ melting“ and „ freezing“ kinetics of the magnetostructural phase transition in B2-ordered FeRh epilayers," *Appl. Phys. Lett.*, vol. 104, p. 232407, 2014.
- [6] M. P. Annaorazov, K. a. Asatryan, G. Myalikgulyev, S. a. Nikitin, A. M. Tishin, and A. L. Tyurin, "Alloys of the Fe-Rh system as a new class of working material for magnetic refrigerators," *Cryogenics*, vol. 32, no. 10, pp. 867–872, 1992.
- [7] M. P. Annaorazov, S. A. Nikitin, A. L. Tyurin, K. A. Asatryan, and A. K. Dovletov, "Anomalously high entropy change in FeRh alloy," *J. Appl. Phys.*, vol. 79, pp. 1689–1695, 1996.
- [8] G. Shirane, C. W. Chen, P. A. Flinn, and R. Nathans, "Hyperfine fields and magnetic moments in the Fe-Rh system," *J. Appl. Phys.*, vol. 34, no. 4, pp. 1044–1045, 1963.
- [9] R. Barua, F. Jiménez-Villacorta, and L. H. Lewis, "Predicting magnetostructural trends in FeRh-based ternary systems," *Appl. Phys. Lett.*, vol. 103, no. 10, p. 102407, Sep. 2013.
- [10] J.-U. Thiele, M. Buess, and C. H. Back, "Spin dynamics of the antiferromagnetic-to-ferromagnetic phase transition in FeRh on a sub-picosecond time scale," *Appl. Phys. Lett.*, vol. 85, no. 14, pp. 2857–2859, 2004.
- [11] J.-U. Thiele, S. Maat, J. L. Robertson, and E. E. Fullerton, "Magnetic and structural properties of FePt-FeRh exchange spring films for thermally assisted magnetic recording media," *IEEE Trans. Magn.*, vol. 40, no. 4, pp. 2537–2542, 2004.
- [12] X. Marti *et al.*, "Room-temperature antiferromagnetic memory resistor," *Nat. Mater.*, vol. 13, pp. 367–374, 2014.
- [13] T. Moriyama, N. Matsuzaki, K.-J. Kim, I. Suzuki, T. Taniyama, and T. Ono, "Sequential write-read operations in FeRh antiferromagnetic memory," *Appl. Phys. Lett.*, vol. 107, p. 122403, 2015.
- [14] C. Le Graët *et al.*, "Temperature controlled motion of an antiferromagnet-ferromagnet interface within a dopant-graded FeRh epilayer," *APL Mater.*, vol. 3, no. 4, p. 41802, 2015.
- [15] M. Loving, F. Jimenez-Villacorta, B. Kaeswurm, D. A. Arena, C. H. Marrows, and L. H. Lewis, "Structural evidence for stabilized ferromagnetism in epitaxial FeRh nanoislands," *J. Phys. D Appl. Phys.*, vol. 46, pp. 162002–6, 2013.
- [16] H. Y. Y. Ko, T. Suzuki, N. N. Phuoc, and J. Cao, "Fabrication and characterization of FeRh nanoparticles," *J. Appl. Phys.*, vol. 103, p. 07D508, 2008.
- [17] I. Suzuki, T. Naito, M. Itoh, and T. Taniyama, "Barkhausen-like antiferromagnetic to ferromagnetic phase transition driven by spin polarized current," *Appl. Phys. Lett.*, vol. 107, p. 82408, 2015.
- [18] V. Uhlir, J. A. Arregi, and E. E. Fullerton, "Colossal magnetic phase transition asymmetry in mesoscale FeRh stripes," *Nat. Commun.*, vol. 7, p. 13113, 2016.
- [19] N. V. Baranov and E. A. Barabanova, "Electrical resistivity and magnetic phase transitions in modified FeRh compounds," *J. Alloys Compd.*, vol. 219, pp. 139–148, 1995.
- [20] S. Maat, J.-U. Thiele, and E. E. Fullerton, "Temperature and field hysteresis of the antiferromagnetic-to-ferromagnetic phase transition in epitaxial FeRh films," *Phys. Rev. B*, vol. 72, no. 21, p. 214432, 2005.
- [21] K. Nishimura, Y. Nakazawa, L. Li, and K. Mori, "Magnetocaloric Effect of $\text{Fe}(\text{Rh}_{1-x}\text{Pd}_x)$ Alloys," *Mater. Trans.*, vol. 49, no. 8, pp. 1753–1756, 2008.
- [22] N. Matsuzaki *et al.*, "Current induced antiferro – ferromagnetic transition in FeRh nanowires," *Jpn. J. Appl. Phys.*, vol. 54, p. 73002, 2015.
- [23] P. Kushwaha, A. Lakhani, R. Rawat, and P. Chaddah, "Low-temperature study of field-induced antiferromagnetic-ferromagnetic transition in Pd-doped Fe-Rh," *Phys. Rev. B*, vol. 80, p. 174413, 2009.
- [24] C. Baldasseroni *et al.*, "Temperature-driven nucleation of ferromagnetic domains in FeRh thin films," *Appl. Phys. Lett.*, vol. 100, p. 262401, 2012.
- [25] C. Baldasseroni *et al.*, "Temperature-driven growth of antiferromagnetic domains in thin-film FeRh," *J. Phys. Condens. Matter*, vol. 27, p. 256001, 2015.

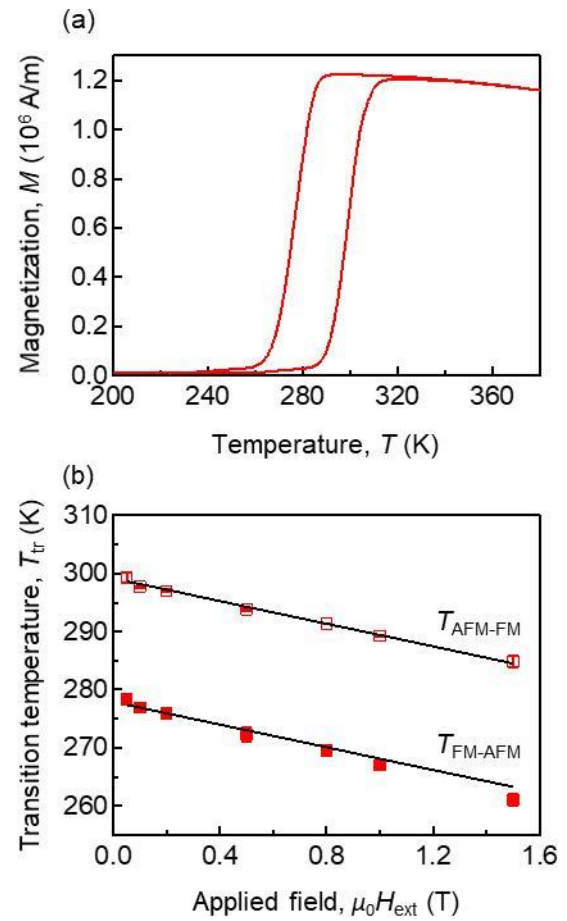


Fig. 1. (a) Temperature-driven hysteresis loop of magnetization of the unpatterned FeRhPd/MgO (001) film under an in-plane external magnetic field of 0.1 T. (b) Phase transition temperatures against external magnetic field. Transition temperatures were determined by peak positions of magnetization against temperature under a constant external magnetic field. Transition temperatures during heating (T_{AFM-FM} , open symbols) and cooling (T_{FM-AFM} , closed symbols) processes are shown. Lines of best fit (solid lines) have the same slope of

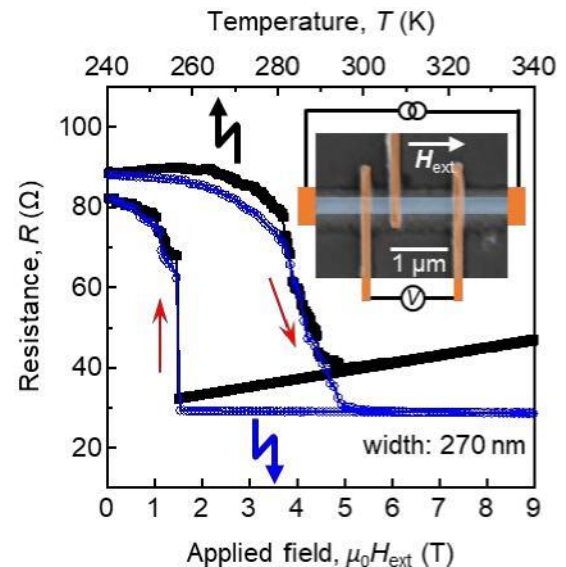


Fig. 2. Resistance measurements on a submicron wire of FeRhPd/MgO (001) as a function of temperature (black, closed square symbols) and in-plane

magnetic field (blue, open circle symbols). The temperature-driven hysteresis loop was measured without applying a magnetic field and the field-driven one was done at a constant temperature of 240.0 K. Red arrows shows the sweep direction of temperature and magnetic field. The inset shows a SEM image of the wire.

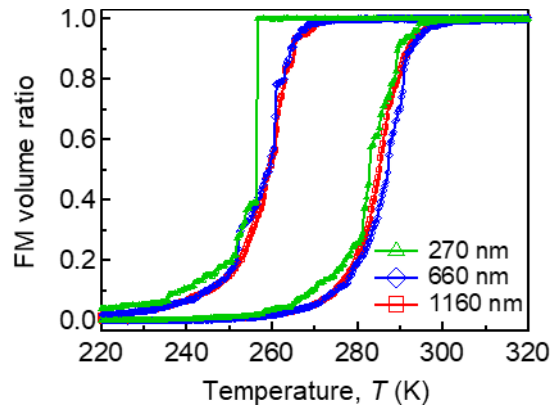


Fig. 3. Ferromagnetic (FM) phase volume ratio of submicron wires of FeRhPd/MgO (001) against temperature. FM phase volume ratio on each wire was calculated from four-terminal resistance measurement on 270 nm wide wire and two-terminal resistance measurements on 660 nm and 1160 nm wide ones. All measurements were performed without an external magnetic field.